Main-Group Chemistry Hot Paper

How to cite: *Angew. Chem. Int. Ed.* **2022,** *61,* e202115379
International Edition: doi.org/10.1002/anie.202115379
German Edition: doi.org/10.1002/ange.202115379

Formation and Reactivity of a Hexahydridosilicate $[SiH_6]^{2-}$ Coordinated by a Macrocycle-Supported Strontium Cation

*Thomas Höllerhage, Priyabrata Ghana, Thomas P. Spaniol, Ambre Carpentier, Laurent Maron, Ulli Englert, and Jun Okuda**

In memory of Robert H. Grubbs

Abstract: *The cationic benzyl complex [(Me$_4$TACD)Sr(CH$_2$Ph)][A] (Me$_4$TACD = 1,4,7,10-tetramethyltetraazacyclododecane; A = B(C$_6$H$_3$-3,5-Me$_2$)$_4$) reacted with two equivalents of phenylsilane to give the bridging hexahydridosilicate complex [(Me$_4$TACD)$_2$Sr$_2$(thf)$_4$(μ-κ^3:κ^3-SiH$_6$)][A]$_2$ (**3a**). Rapid phenyl exchange between phenylsilane molecules is assumed to generate monosilane SiH$_4$ that is trapped by two strontium hydride cations [(Me$_4$TACD)SrH(thf)$_x$]$^+$. Complex **3a** decomposed in THF at room temperature to give the terminal silanide complex [(Me$_4$TACD)Sr(SiH$_3$)(thf)$_2$][A], with release of H$_2$. Upon reaction with a weak Brønsted acid, CO$_2$, and 1,3,5,7-cyclooctatetraene SiH$_4$ was released. The reaction of a 1:2 mixture of cationic benzyl and neutral dibenzyl complex with phenylsilane gave the trinuclear silanide complex [(Me$_4$TACD)$_3$Sr$_3$(μ$_2$-H)$_3$(μ$_3$-SiH$_3$)$_2$][A], while ^{n}OctSiH$_3$ led to the trinuclear (n-octyl)pentahydridosilicate complex [(Me$_4$TACD)$_3$Sr$_3$(μ$_2$-H)$_3$(μ$_3$-SiH$_5$^{n}Oct)][A].*

Introduction

Hypercoordinate ("hypervalent") silicates $[SiX_5]^-$ and $[SiX_6]^{2-}$ (X = H, halogen, alkyl) are of fundamental interest in understanding of structure and bonding[1] as well as in synthetic applications due to enhanced nucleophilicity of the substituent X.[2] For X = H, however, there is surprisingly little information in the literature.[3] While $[SiH_5]^-$ has been studied in the gas phase,[4] only two examples of structurally characterized compounds with $[SiH_6]^{2-}$ have been reported: Häussermann et al. obtained $K_2[SiH_6]$ by high pressure solid state synthesis from a mixture of KH/Si/H_2 or K_4Si_4/H_2,[5] while Tilley et al. prepared the dinuclear ruthenium(II) complex $[(PhBP^{Ph}_3)Ru]_2[\mu\text{-}\eta^4,\eta^4\text{-}SiH_6]$ ($PhBP^{Ph}_3$ = PhB(CH$_2$PPh$_2$)$_3$) by substitution of a diarylsilane σ-adduct at a ruthenium hydride.[6] In addition, a limited number of mixed hydrido silicates have been reported, including the structurally characterized dihydridotriphenylsilicate $[Ph_3SiH_2]^-$[7] and a remarkably inert calix[4]pyrrole hydrido silicate.[8] The ability of tetracoordinate silicon to expand its coordination number is also important in alkaline-earth metal catalysis involving hydrosilanes, where stepwise nucleophilic substitution via a hypercoordinate silicate may take place instead of classical σ-bond metathesis.[9] Furthermore, in the context of understanding dihydrogen uptake and release in the hydrogen storage material $K_4Si_4/KSiH_3$,[10] it is of interest to study the relationship between low valent systems SiH_3^-, SiH_2,[11] and $[Si_4]^{4-}$ and hypercoordinate hydridosilicates $[SiH_5]^-$ and $[SiH_6]^{2-}$ as hydride adducts of monosilane SiH_4. Here we show that the previously reported reactive hydrido cation of strontium $[(Me_4TACD)SrH(thf)_x]^+$ (Me$_4$TACD = 1,4,7,10-tetramethyltetraazacyclododecane)[12] forms a hexahydridosilicate complex $[(Me_4TACD)_2Sr_2(thf)_4(\mu\text{-}\kappa^3\text{:}\kappa^3\text{-}SiH_6)][B(C_6H_3\text{-}3,5\text{-}Me_2)_4]_2$ (**3a**) containing a bridging $[SiH_6]^{2-}$ anion. Isolation of **3a** allowed the study of its structure, bonding, and reactivity.

Results and Discussion

When a yellow solution of $[(Me_4TACD)Sr(CH_2Ph)][B(C_6H_3\text{-}3,5\text{-}Me_2)_4]$ (**2a**)[12] in THF-d_8 was reacted with excess $PhSiH_3$ at room temperature, immediate discoloration was observed. Upon work-up, $[(Me_4TACD)_2Sr_2(thf)_4(\mu\text{-}\kappa^3\text{:}\kappa^3\text{-}SiH_6)][B(C_6H_3\text{-}3,5\text{-}Me_2)_4]_2$ (**3a**) containing a bridging hexahydridosilicate $[SiH_6]^{2-}$ anion between two strontium centers was isolated (Scheme 1). σ-Bond metathesis of the benzyl complex with $PhSiH_3$ to give the reactive intermediate $[(Me_4TACD)SrH(thf)_x]^+$ and $Ph(PhCH_2)SiH_2$ can be inferred as the first step. Fast redistribution[9b,13] of $PhSiH_3$ in the presence of $[(Me_4TACD)SrH(thf)_x]^+$ further gives $Ph_2(PhCH_2)SiH$ and SiH_4. The latter reacts with two equiv. of $[(Me_4TACD)SrH(thf)_x]^+$ to give **3a**, although low temperature monitoring of the reaction mixture remained inconclusive. The ^{1}H and ^{29}Si NMR spectra of the high-boiling residue of the reaction mixture indicated the formation of secondary and tertiary silanes $R_xR'_ySiH_{(4\text{-}x\text{-}y)}$ (R = PhCH$_2$,

[*] T. Höllerhage, Dr. P. Ghana, Dr. T. P. Spaniol, Prof. Dr. U. Englert, Prof. Dr. J. Okuda
Institute of Inorganic Chemistry, RWTH Aachen University
Landoltweg 1, 52056 Aachen (Germany)
E-mail: jun.okuda@ac.rwth-aachen.de
A. Carpentier, Prof. Dr. L. Maron
CNRS, INSA, UPS, UMR 5215, LPCNO
Université de Toulouse
135 avenue de Rangueil, 31077 Toulouse (France)

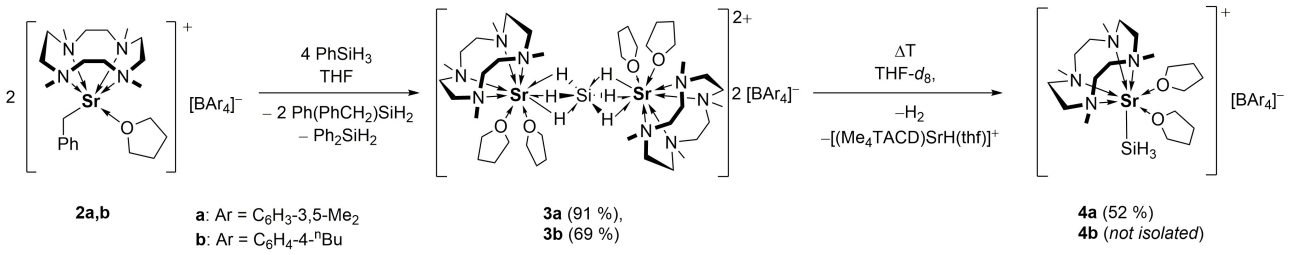

Scheme 1. Synthesis of hydridosilicate complexes **3a**,**b** and thermal decomposition to silanides **4a**,**b**.

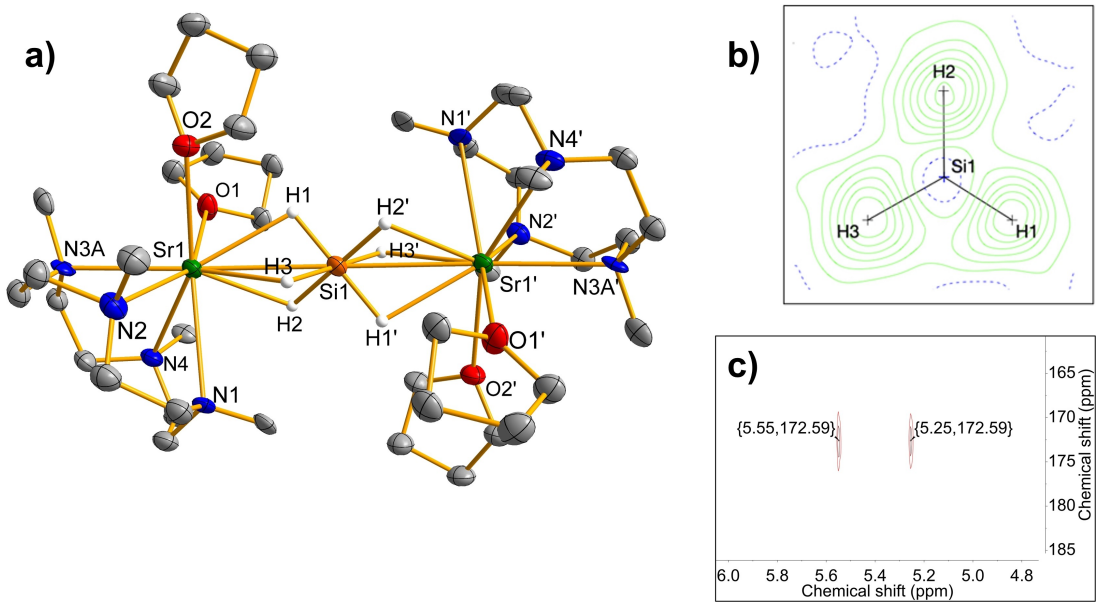

Figure 1. a) Displacement ellipsoid plot (30% probability) of the dinuclear cation in the crystal structure of **3b**; only H atoms in the hydridosilicate are shown.[28] b) Difference Fourier map before including the three symmetrically independent H atoms of the hydridosilicate into the structure model. Green contour lines correspond to positive electron density and have been drawn at 0.1 e Å^{-3} intervals. c) Cutout of the ^{1}H–^{29}Si HMBC NMR spectrum of **3b** at −40 °C.

x = 0, 1 or 2; R′ = Ph, y = 0, 1, or 2; x + y = 1, 2, or 3). When **3a** was heated in the presence of an excess of $PhSiH_3$ the formation of Ph_2SiH_2 and SiH_4 was observed but no Ph_3SiH. Similar redistribution to SiH_4 was observed in the synthesis of $[(BDI)CaH]_2$ (BDI = CH[C(CH$_3$)NDipp]$_2$, Dipp = 2,6-diisopropylphenyl).[14]

Compound **3a**, albeit crystalline, did not meet the requirements for reliably elucidating the hydrogen atom geometry by single crystal X-ray diffraction. Solid **3a** contained seven non-coordinated and less well-defined THF molecules in the asymmetric unit (see Supporting Information). More suitable crystals of $[(Me_4TACD)_2Sr_2(thf)_4(\mu\text{-}\kappa^3\text{:}\kappa^3\text{-}SiH_6)][B(C_6H_4\text{-}4\text{-}^nBu)_4]_2$ (**3b**) were obtained using a related anion $[B(C_6H_4\text{-}4\text{-}^nBu)_4]^-$ starting from $[(Me_4TACD)Sr(CH_2Ph)][B(C_6H_4\text{-}4\text{-}^nBu)_4]$ (**2b**). **3b** crystallizes as a dinuclear complex with the $[SiH_6]^{2-}$ bridging between two strontium ions; the silicon atom resides on a crystallographic center of inversion (Figure 1a). Each metal cation is coordinated by two THF ligands in addition to the κ^4-Me$_4$TACD macrocycle. The quality of the diffraction data allowed the unambiguous assignment of local electron density maxima to the hydridic atom sites (Figure 1b) and free refinement of their positional parameters and individual isotropic displacement parameters. The bridging hydridosilicate ligand shows octahedral coordination about silicon, with the Si–H bond lengths in the range of 1.51(2) to 1.588(19) Å. Silicon and alkaline earth cations connect to opposite triangular faces of the octahedron; Sr–H bonds between 2.39(2) and 2.44(2) Å are equidistant within error. The hydride polyhedron about silicon is slightly elongated in the direction of Sr···Sr vector. The intra-cation separation between the strontium sites amounts to 6.1140(4) Å; a similar distance of 6.0919(9) Å was found from the less precise structural study on **3a**, suggesting an analogous bonding situation in both crystalline solids. The Si–H bond lengths in **3a** are considerably shorter than the Si–H bond lengths observed in $[(PhBP^{Ph}_3)Ru]_2[\mu\text{-}\eta^4,\eta^4\text{-}SiH_6]$ (1.69 to 1.79 Å).[6] For the computationally optimized structure of K_2SiH_6, Si–H bond lengths of 1.62 Å were reported.[5]

DFT calculations (B3PW91 functional) including dispersion corrections were carried out to describe the bonding in complex **3a**. The optimized structure is in fair agreement

with the experimental one (see Supporting Information) with the Sr–H bonds well reproduced (2.42 Å). The bond lengths around silicon were found to be complicated to reproduce computationally (1.59 and 1.62 Å compared with 1.51 and 1.59 Å experimentally). This is probably due to a Basis Set Superposition Error (BSSE), since large basis sets had to be used to describe the hypervalent structure of silicon. However, the maximum deviation is 0.08 Å and therefore bonding analysis was carried out using Natural Bonding Orbital (NBO) method (see Supporting Information). The six Si–H bonds were found to be strongly polarized toward hydrogen (72 to 74 %) and involve overlap between an *spd* hybrid atomic orbital (18 % s, 50 % p, 32 % d) on silicon and a 1 s orbital of hydrogen. This is in line with average computed Si–H Wiberg Bond Indices (WBIs) of 0.6. At the second order, the Si–H bonds appear to be delocalized toward strontium in line with the formation of 3 center-2 electron (3c–2e) bonds explaining the WBI value of 0.15 for Sr–H as well as WBI of 0.18 for Sr–Si.

3a and **3b** are unstable in THF-d_8 above 0 °C (see below) and were therefore characterized by low temperature NMR studies. The hydridosilicate ligand gives a broad resonance in the ^{1}H NMR spectrum above 0 °C that becomes a sharp singlet at −20 °C and below. At −40 °C resonances are observable in the ^{29}Si–^{1}H HSQC and ^{29}Si-^{1}H HMBC spectra that could not be detected above this temperature. Despite numerous attempts, direct measurements such as DEPT20 or DEPT45 experiments did not show any ^{29}Si resonances. In the ^{29}Si-^{1}H HMBC spectrum, the $[SiH_6]^{2-}$ anion gives rise to a doublet at $\delta = 172.6$ ppm with a coupling constant of $^1J_{SiH} = 118$ Hz (Figure 1c). In comparison, the ^{29}Si resonance at $\delta = 162$ ppm of $[(PhBP^{Ph}_3)Ru]_2[\mu\text{-}\eta^4,\eta^4\text{-}SiH_6]$ is slightly upfield shifted and the observed coupling constant was $^1J_{SiH} = 74.5$ Hz.[6] These findings as well as the shorter Si–H bond lengths in **3b** indicate that the $[SiH_6]^{2-}$ shows an expectedly more ionic bonding to the strontium cations as opposed to $[(PhBP^{Ph}_3)Ru]_2[\mu\text{-}\eta^4,\eta^4\text{-}SiH_6]$ with stronger ruthenium-hydride interactions.[6] Characteristic Si–H stretching frequencies were observed for **3a** at $\nu = 1717$ cm^{-1} in the ATR-IR spectrum and $\nu = 1792$ cm^{-1} in the Raman spectrum. These wavenumbers are similar to those observed in K_2SiH_6 ($\nu = 1739$ cm^{-1}, Raman) and $[(PhBP^{Ph}_3)Ru]_2[\mu\text{-}\eta^4,\eta^4\text{-}SiH_6]$ ($\nu = 1746$ cm^{-1}, IR in Nujol). The deuterated isotopomer **3a-d_6**, prepared analogously from **2a** and $PhSiD_3$, shows an Si–D stretching absorption in the ATR-IR spectrum at $\nu = 1247$ cm^{-1} ($\nu_H/\nu_D = 1.44$). The Si–H vibrational frequency as well as the ^{29}Si NMR chemical shift were also obtained computationally. A stretching band with strong IR intensity at $\nu = 1710$ cm^{-1} was calculated, which is in good agreement with the observed experimental frequency. The ^{29}Si NMR chemical shift was computed to be $\delta = 208$ ppm, with an overestimation of 10 %. This is in line with errors reported in the literature.[15]

When a solution of **3a**,**b** in THF-d_8 was left standing above 0 °C, H_2 evolved and in the ^{1}H NMR spectrum the broad resonance of $[SiH_6]^{2-}$ gave way to a new sharp signal at $\delta = 5.88$ ppm over the course of 4 h, in agreement with the chemical shift for the hydride ligand in $[(Me_4TACD)SrH(thf)_x]^+$.[12] No resonance for SiH_4 was detected in the reaction mixture as shown by ^{1}H NMR spectra, ^{29}Si–^{1}H HSQC, and ^{29}Si–^{1}H HMBC measurements at 23 °C. Cooling the decomposition mixture of **3b** to −40 °C showed a single resonance at $\delta = -130.8$ ppm, in the region expected for a silanide anion SiH_3^- coordinated to an electropositive metal (see below).[3c,16]

These observations were supported by X-ray diffraction analysis of colorless single crystals, which grew from the decomposition mixture of **3a** and identified as the terminal silanide complex $[(Me_4TACD)Sr(SiH_3)(thf)_2][B(C_6H_3\text{-}3,5\text{-}Me_2)_4]$ (**4a**) (Figure 2). After an initial structure model was established, the most disagreeable diffraction intensities were consistently stronger than their calculated counterparts. The metric of the unit cell of **4a** allowed approximate non-crystallographic rotation about the [0 1 −1] direction as twin law, and the presence of many partially overlapped intensities necessarily limits the precision of the diffraction experiment. Despite these limitations, local electron density maxima associated with the hydrogen atoms of a disordered terminal SiH_3 moiety could be identified (see for further details in the Supporting Information). Based on a search in the CSD,[17] the hydrogen sites in this group were constrained to a distance Si–H = 1.38 Å (see Supporting Information).

While there are several examples of structurally characterized alkali metal,[3c,16] lanthanide,[18] and transition metal complexes[19] containing the SiH_3^- anion, **4a** appears to be the first structurally authenticated complex with the SiH_3^- anion coordinated to an alkaline earth metal.

When one equivalent of **2a** were reacted with $PhSiH_3$ in the presence of two equivalents of the neutral benzyl **1**, the trinuclear cluster $[(Me_4TACD)_3Sr_3(\mu\text{-}H)_3(\mu_3\text{-}SiH_3)_2][B(C_6H_3\text{-}3,5\text{-}Me_2)_4]$ (**5**) was isolated in 62 % yield (Scheme 2). H_2 gas evolution during the formation of **5** suggests that $[(Me_4TACD)Sr(SiH_3)(thf)_x]^+$ is formed by reductive elimination of H_2 from an undetected intermediate $[(Me_4TACD)Sr(SiH_5)(thf)_x]^+$, by analogy to the formation of **4** from **3**.

Cluster **5** can formally be regarded as a combination of two units of $[(Me_4TACD)Sr(SiH_3)H]$ and one unit of

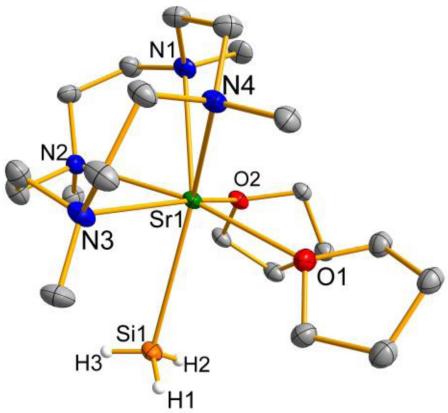

Figure 2. Displacement ellipsoid plot (30 % probability) of the cationic complex with a terminal silanide ligand in **4a**; only H atoms in the majority conformer of the SiH_3 group are shown.[28]

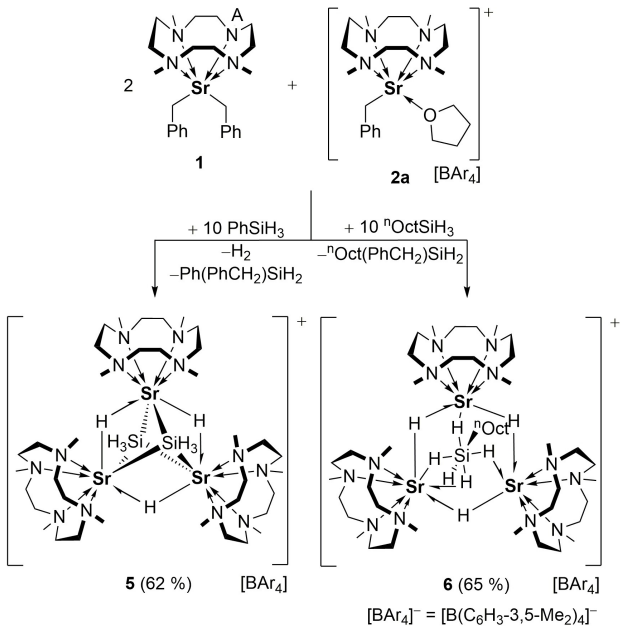

Scheme 2. Synthesis of hydride-silanide cluster **5** and hydride-*n*-octylhydridosilicate cluster **6**.

$[(Me_4TACD)SrH]^+$ or of two units of $[(Me_4TACD)Sr(SiH_3)]^+$ and one unit of $[(Me_4TACD)SrH_3]^-$, thus as a derivative of $[(Me_4TACD)_3Sr_3H_5]^+$.

According to the single crystal diffraction analysis, the cation in **5** contains a triangular strontium core of distorted D_{3h}-symmetry with three Sr···Sr edges between 4.0968(4) and 4.1707(5) Å bridged by H atoms. The Sr_3 plane is capped by two SiH_3 units on each side (Figure 3).

As for complex **3b**, DFT calculations were also carried out for complex **5** (see Supporting Information). At the NBO level, Sr–H as well as Sr–Si bonds were found. Both bonds are strongly polarized toward either H (85 %) or Si (88–90 %). At the second order, the Sr–H bonds are found to delocalize onto the adjacent Sr in line with the formation of 3c–2e Sr–H–Sr bonds. The Sr–H bonds involve an overlap between an *spd* hybrid atomic orbital on strontium and the 1s orbital of hydrogen. A similar situation is found for the Sr–Si bonds formed by the overlap of an *spd* hybrid orbital (9 % s, 40 % p, 51 % d) on strontium and an *sp* hybrid orbital (60 % s, 40 % p) on silicon. This bonding situation is in line with the computed Sr–H and Sr–Si WBI of 0.35 and 0.30, respectively.

In the ^{1}H NMR spectrum of **5** the hydride ligands appear at $\delta = 5.86$ ppm and the SiH_3^- ligands at $\delta = 2.07$ ppm, both in the expected chemical shift ranges for these ligands.[3c,12,16,20] Additionally, spin-spin coupling ($^3J_{HH} = 1.7$ Hz) between the hydride and SiH_3^- ligands in **5** was observed. **5** is relatively stable in THF-d_8 solution and no decomposition was observed at room temperature within 48 h, in contrast to the related Me_4TACD-supported strontium hydride complexes **3**, **6** and $[(Me_4TACD)_3Sr_3(\mu\text{-}H)_4(thf)][B(C_6H_3\text{-}3,5\text{-}Me_2)_4]_2$.[12] In the ATR-IR spectrum the Si–H stretching absorption of **5** was observed at $\nu = 1923$ cm^{-1}. The deuterated isotopomer **5-d_9** prepared analogously to **5** using $PhSiD_3$, shows a resonance for Sr–D at $\delta = 5.95$ ppm and for SiD_3^- at $\delta = 2.01$ ppm in the ^{2}H NMR spectrum.

The observation that the in situ generated $[(Me_4TACD)SrH(thf)_x]^+$ fragment strongly interacts with silanes prompted us to use ^{n}OctSiH$_3$ as a hydride source to avoid aryl group redistribution at the silicon center. When two equiv. of **1** and one equiv. of **2a** were reacted with ^{n}OctSiH$_3$, instantaneous reaction was observed. Single-crystal structure analysis of the reaction product revealed formation of the trinuclear cluster $[(Me_4TACD)_3Sr_3(\mu\text{-}H)_3(\mu_3\text{-}SiH_5{}^nOct)][B(C_6H_3\text{-}3,5\text{-}Me_2)_4]$ (**6**). The intermolecular Sr···Sr distances between 4.0908(4) Å and 4.1294(4) Å in **6** can be compared with those in **5**, but in **6** the Sr_3 triangle is

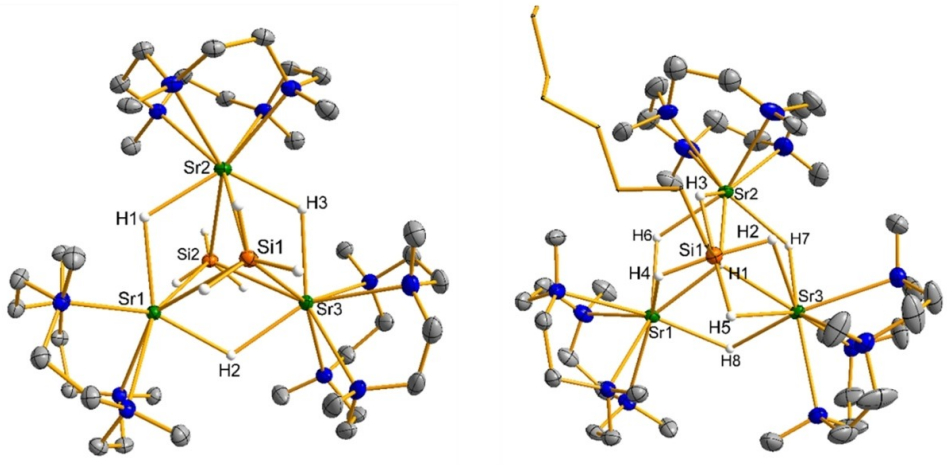

Figure 3. Displacement ellipsoid plots (30 % probability) of the trinuclear cation in crystals of **5** (left) and **6** (right). Only hydride ligands and H atoms of SiH_3^- or $[^nOctSiH_5]^{2-}$ ligands are shown.[28]

bridged by a hypercoordinate $[^{n}OctSiH_5]^{2-}$ unit. Considering the latter as an adduct of two hydrides to $^{n}OctSiH_3$, complex **6** can be regarded as made up by two neutral $[(Me_4TACD)SrH_2]$ fragments, one cationic $[(Me_4TACD)SrH]^+$ moiety and one $^{n}OctSiH_3$ molecule. To the best of our knowledge, an (alkyl)pentahydridosilicate has so far not been reported.

In the ^{1}H NMR spectrum of **6** in THF-d_8 the hydride and $[^{n}OctSiH_5]^{2-}$ ligands give a broad resonance ($\delta = 5.66$ ppm) at room temperature. In agreement with C_s-symmetry, the two resonances should give a pattern of five signals in a 2:2:2:1:1 ratio. Although below −40 °C the resonances sharpen, a complicated pattern of resonances appears at −80 °C, suggesting a less symmetric structure resulting from frozen fluxionality of the hydride ligands. A ^{29}Si-^{1}H HSQC NMR measurement at −80 °C gave a ^{29}Si resonance at $\delta =$ 112.4 ppm. It appears that the exchange of hydride ligands is too fast above this temperature to obtain 2D NMR spectra. As in the case of **3a**, DEPT20 and DEPT45 measurements were unsuccessful. In the ATR-IR spectrum of **6** a characteristic Si–H stretching frequency was observed at $\nu =$ 1703 cm^{-1}. DFT calculations were carried out on complex **6** (see Supporting Information). NBO analysis indicates the presence of Si–H and Sr–H bonds, which like complexes **3** and **5**, are strongly polarized toward hydrogen (73 to 85 %). The Sr–H bonds are found at the second order donor–acceptor level to be delocalized onto the adjacent strontium atom, in line with the presence of 3c–2e Sr–H–Sr bonds as found in complex **5**. The associated Sr–H WBI are 0.35 in line with the Sr–H WBI found for complex **5**. The Si–H bonds are also found to be slightly delocalized toward strontium but the Si–H WBI are around 0.5, the values for Sr–H are approximately 0.1. The latter delocalization leads to a Sr–Si WBI of 0.1–0.18. These values are similar to those found for complex **3b**. The bonding situation in complex **6** can be considered a superposition of the bonding situation found in complexes **3b** and **5**.

To explore the nature of the $[SiH_6]^{2-}$ anion in **3a**, the reactivity toward a weak Brønsted acid, CO_2 as an electrophile, and 1,3,5,7-cyclooctatetraene (COT) as a mild oxidant was investigated (Scheme 3). Reactivity studies were carried out with **3a** rather than **3b** due to the more straightforward synthesis of **3a**, and easier isolation of the products with the $[B(C_6H_3\text{-}3,5\text{-}Me_2)_4]^-$ anion. Thus **3a** reacted with two equivalents of the weak Brønsted acid $[NEt_3H][B(C_6H_3\text{-}3,5\text{-}Me_2)_4]$ to release both H_2 and SiH_4 and cleanly gave the dication $[(Me_4TACD)Sr(thf)_2][B(C_6H_3\text{-}3,5\text{-}Me_2)_4]_2$ (**7**),[12] which was identified in the ^{1}H NMR spectrum of the protonolysis mixture in THF-d_8. With CO_2 (1 bar), **3a** quickly reacted at 0 °C to give the dinuclear formate complex $[(Me_4TACD)_2Sr_2(\mu\text{-}OCHO)_2][B(C_6H_3\text{-}3,5\text{-}Me_2)_4]_2$ (**8**) with concomitant release of SiH_4. **8** was isolated and fully characterized including by single crystal diffraction analysis. The NMR spectra show the characteristic resonances for the formate ligand at $\delta(^1H) = 8.47$ ppm and $\delta(^{13}C) = 169.3$ ppm, slightly downfield shifted compared to its isostructural calcium homolog ($\delta(^1H) = 8.37$ ppm and $\delta(^{13}C) =$ 167.4 ppm).[21] **3a** reacted with 1,3,5,7-cyclooctatetraene under release of H_2 and SiH_4 to give the dinuclear complex $[(Me_4TACD)_2Sr_2(\mu,\eta^8\text{:}\eta^8\text{-}COT)][B(C_6H_3\text{-}3,5\text{-}Me_2)_4]_2$ (**9**). The cyclooctatetraenediyl ligand gives rise to resonances at $\delta(^1H) = 6.46$ ppm and $\delta(^{13}C) = 92.6$ ppm in the NMR spectra. Heavier alkaline earth metals containing the cyclooctatetraenediyl ligand are well-known in the literature.[22] The

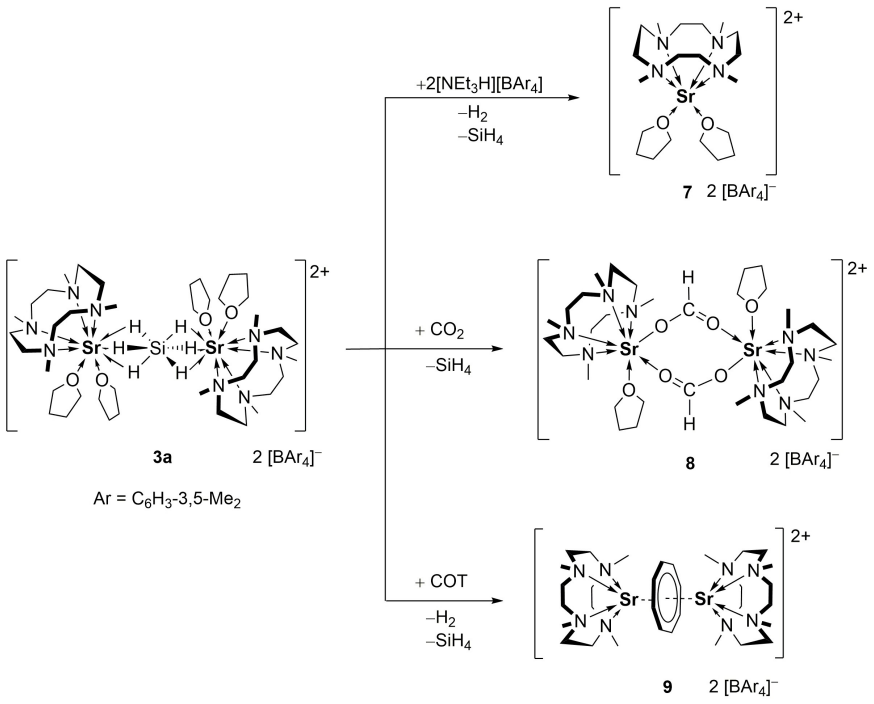

Scheme 3. Reactivity of hydridosilicate complex **3a**.

calcium hydride complex $[(BDI)CaH]_2$ has been reported by Hill et al. to form a bridging COT complex with release of H_2.[23]

When compared with the thermolysis of **3a**, which releases H_2 but no SiH_4, it appears that external reagents follow a distinct pathway that leads to fast dissociation of **3a** into two $[(Me_4TACD)SrH(thf)_x]^+$ and SiH_4. Thus, the reactivity pattern of **3a** is best rationalized by regarding the complex as two SiH_4-masked nucleophilic hydride cations $[(Me_4TACD)SrH]^+$.

Conclusion

The highly reactive strontium hydride cations $[(Me_4TACD)SrH(thf)_x]^+$ enable stabilization of hexahydridosilicate, silanide and (n-alkyl)pentahydridosilicate anions. The highly nucleophilic character of the strontium hydride allows these rare silicon anions to be isolated. When compared to lighter alkaline earth metal congeners magnesium and calcium, strontium with its large ionic radius (ionic radii for c.n. = 6: 0.86 Å for Mg, 1.14 Å for Ca, 1.32 Å for Sr),[24] and higher electropositivity (EN = 1.30 for Mg, 1.00 for Ca, 0.95 for Sr)[25] exhibits more polar interactions and pronounced ligand lability. As a result, we have previously observed that the strontium hydride cation $[(Me_4TACD)SrH(thf)_x]^+$ readily undergoes redistribution (Schlenk equilibrium) in THF to give $[(Me_4TACD)Sr]^{2+}$ and $[(Me_4TACD)SrH_2]$ (isolable as the trinuclear tetrahydride dication $[(Me_4TACD)_3Sr_3H_4]^{2+}$).[12] In a mixed calcium–strontium system, this high lability and nucleophilicity results in hydride transfer from strontium to calcium.[12] The results reported here further underline the potential for highly reactive complexes of the electropositive heavy alkaline earth metals to exhibit unusual reactivity patterns,[14,20e,26] some aspects of which have recently been ascribed to non-negligible contributions of d-orbitals in metal–ligand bonding.[27]

The isolation of thermally sensitive hexahydridosilicate **3** occurred due to the fast redistribution of phenylsilane catalyzed by $[(Me_4TACD)SrH(thf)_x]^+$ to give monosilane. When the more inert n-alkyl hydrosilane ^{n}OctSiH$_3$ was present, $[(Me_4TACD)_3Sr_3H_3]^{3+}$ core stabilized an alkyl-substituted pentahydridosilicate $[^n OctSiH_5]^{2-}$. While reactions of **3** with a Brønsted acid, an electrophile such as CO_2, and a mild oxidant all reflect the inherent reactivity of $[(Me_4TACD)SrH(thf)_x]^+$, thermal decomposition gave the terminal silanide **4**, which may have formed by reductive elimination of H_2 from the hypothetical pentahydridosilicate intermediate $[(Me_4TACD)Sr(SiH_5)]^+$. In the context of hydrogen storage systems such as $K_4Si_4/KSiH_3$,[10] it would be interesting to further explore the reductive elimination of H_2 from these hydrogen-rich silicon compounds.

Acknowledgements

We thank the Deutsche Forschungsgemeinschaft for financial support, Prof. A. Filippou for help with vibrational spectra, Dr. G. Fink for NMR spectroscopic measurements, F. Ritter and Dr. L. J. Morris for X-ray diffraction measurements. L.M. is member of the Institut Universitaire de France and thanks the Alexander von Humboldt foundation for a scholarship. CalMip is acknowledged for a generous grant of computing time. Open Access funding enabled and organized by Projekt DEAL.

Conflict of Interest

The authors declare no conflict of interest.

Data Availability Statement

The data that support the findings of this study are available from the corresponding author upon reasonable request.

Keywords: alkaline earth metal · hydride complex · hydridosilicate · silanide · strontium

[1] a) S. Noury, B. Silvi, R. J. Gillespie, *Inorg. Chem.* **2002**, *41*, 2164–2172; b) S. C. A. H. Pierrefixe, F. M. Bickelhaupt, *Struct. Chem.* **2007**, *18*, 813–819; c) T. H. Dunning, L. T. Xu, J. V. K. Thompson, *J. Phys. Chem. A* **2021**, *125*, 7414–7424; d) D. L. Wilhite, L. Spialter, *J. Am. Chem. Soc.* **1973**, *95*, 2100–2104; e) E. P. A. Couzijn, A. W. Ehlers, M. Schakel, K. Lammertsma, *J. Am. Chem. Soc.* **2006**, *128*, 13634–13639.

[2] a) C. Chuit, R. J. P. Corriu, C. Reye, J. C. Young, *Chem. Rev.* **1993**, *93*, 1371–1448; b) S. Rendler, M. Oestreich, *Synthesis* **2005**, 1727–1747; c) Y. Nakao, T. Hiyama, *Chem. Soc. Rev.* **2011**, *40*, 4893–4901; d) A. Sugiyama, Y.-y. Ohnishi, M. Nakaoka, Y. Nakao, H. Sato, S. Sakaki, Y. Nakao, T. Hiyama, *J. Am. Chem. Soc.* **2008**, *130*, 12975–12985; e) K. Kikushima, M. Grellier, M. Ohashi, S. Ogoshi, *Angew. Chem. Int. Ed.* **2017**, *56*, 16191–16196; *Angew. Chem.* **2017**, *129*, 16409–16414.

[3] a) P. D. Prince, M. J. Bearpark, G. S. McGrady, J. W. Steed, *Dalton Trans.* **2008**, 271–282; b) P. Jochmann, J. P. Davin, T. P. Spaniol, L. Maron, J. Okuda, *Angew. Chem. Int. Ed.* **2012**, *51*, 4452–4455; *Angew. Chem.* **2012**, *124*, 4528–4531; c) D. Schuhknecht, V. Leich, T. P. Spaniol, I. Douair, L. Maron, J. Okuda, *Chem. Eur. J.* **2020**, *26*, 2821–2825; d) D. Schuhknecht, V. Leich, T. P. Spaniol, J. Okuda, *Chem. Eur. J.* **2018**, *24*, 13424–13427; e) J. Zhou, J. Chu, Y. Zhang, G. Yang, X. Leng, Y. Chen, *Angew. Chem. Int. Ed.* **2013**, *52*, 4243–4246; *Angew. Chem.* **2013**, *125*, 4337–4340.

[4] a) D. J. Hajdasz, R. R. Squires, *J. Am. Chem. Soc.* **1986**, *108*, 3139–3140; b) D. J. Hajdasz, Y. Ho, R. R. Squires, *J. Am. Chem. Soc.* **1994**, *116*, 10751–10760.

[5] K. Puhakainen, D. Benson, J. Nylén, S. Konar, E. Stoyanov, K. Leinenweber, U. Häussermann, *Angew. Chem. Int. Ed.* **2012**, *51*, 3156–3160; *Angew. Chem.* **2012**, *124*, 3210–3214.

[6] M. C. Lipke, T. D. Tilley, *Angew. Chem. Int. Ed.* **2012**, *51*, 11115–11121; *Angew. Chem.* **2012**, *124*, 11277–11283.

[7] M. J. Bearpark, G. S. McGrady, P. D. Prince, J. W. Steed, *J. Am. Chem. Soc.* **2001**, *123*, 7736–7737.

[8] F. Ebner, L. Greb, *J. Am. Chem. Soc.* **2018**, *140*, 17409–17412.

[9] a) F. Buch, J. Brettar, S. Harder, *Angew. Chem. Int. Ed.* **2006**, *45*, 2807–2811; b) D. Schuhknecht, T. P. Spaniol, L. Maron, J. Okuda, *Angew. Chem. Int. Ed.* **2020**, *59*, 310–314; *Angew. Chem.* **2020**, *132*, 317–322; c) J. F. Dunne, S. R. Neal, J.

Engelkemier, A. Ellern, A. D. Sadow, *J. Am. Chem. Soc.* **2011**, *133*, 16782–16785.
[10] a) R. Janot, W. S. Tang, D. Clémençon, J. N. Chotard, *J. Mater. Chem. A* **2016**, *4*, 19045–19052; b) J.-N. Chotard, W. S. Tang, P. Raybaud, R. Janot, *Chem. Eur. J.* **2011**, *17*, 12302–12309.
[11] A. V. Protchenko, K. H. Birjkumar, D. Dange, A. D. Schwarz, D. Vidovic, C. Jones, N. Kaltsoyannis, P. Mountford, S. Aldridge, *J. Am. Chem. Soc.* **2012**, *134*, 6500–6503.
[12] T. Höllerhage, A. Carpentier, T. P. Spaniol, L. Maron, U. Englert, J. Okuda, *Chem. Commun.* **2021**, *57*, 6316–6319.
[13] a) I. Castillo, T. D. Tilley, *J. Am. Chem. Soc.* **2001**, *123*, 10526–10534; b) L. Perrin, L. Maron, O. Eisenstein, T. D. Tilley, *Organometallics* **2009**, *28*, 3767–3775; c) X. Liu, L. Xiang, E. Louyriac, L. Maron, X. Leng, Y. Chen, *J. Am. Chem. Soc.* **2019**, *141*, 138–142; d) Z. Liu, X. Shi, J. Cheng, *Dalton Trans.* **2020**, *49*, 8340–8346; e) T. Li, K. N. McCabe, L. Maron, X. Leng, Y. Chen, *ACS Catal.* **2021**, *11*, 6348–6356.
[14] A. S. S. Wilson, M. S. Hill, M. F. Mahon, C. Dinoi, L. Maron, *Science* **2017**, *358*, 1168.
[15] I. del Rosal, L. Maron, R. Poteau, F. Jolibois, *Dalton Trans.* **2008**, 3959–3970.
[16] D. J. Wolstenholme, P. D. Prince, G. S. McGrady, M. J. Landry, J. W. Steed, *Inorg. Chem.* **2011**, *50*, 11222–11227.
[17] C. R. Groom, I. J. Bruno, M. P. Lightfoot, S. C. Ward, *Acta Crystallogr. Sect. B* **2016**, *72*, 171–179.
[18] N. S. Radu, F. J. Hollander, T. D. Tilley, A. L. Rheingold, *Chem. Commun.* **1996**, 2459–2460.
[19] a) C. Mitzenheim, T. Braun, *Angew. Chem. Int. Ed.* **2013**, *52*, 8625–8628; *Angew. Chem.* **2013**, *125*, 8787–8790; b) S. Schmitzer, U. Weis, H. Kaeb, W. Buchner, W. Malisch, T. Polzer, U. Posset, W. Kiefer, *Inorg. Chem.* **1993**, *32*, 303–309; c) A. A. Zuzek, G. Parkin, *J. Am. Chem. Soc.* **2014**, *136*, 8177–8180; d) L. Hao, *Chem. Commun.* **1998**, 1089–1090.
[20] a) B. Maitland, M. Wiesinger, J. Langer, G. Ballmann, J. Pahl, H. Elsen, C. Färber, S. Harder, *Angew. Chem. Int. Ed.* **2017**, *56*, 11880–11884; *Angew. Chem.* **2017**, *129*, 12042–12046; b) D. Mukherjee, T. Höllerhage, V. Leich, T. P. Spaniol, U. Englert, L. Maron, J. Okuda, *J. Am. Chem. Soc.* **2018**, *140*, 3403–3411; c) C. N. de Bruin-Dickason, T. Sutcliffe, C. Alvarez Lamsfus, G. B. Deacon, L. Maron, C. Jones, *Chem. Commun.* **2018**, *54*, 786–789; d) X. Shi, G. Qin, Y. Wang, L. Zhao, Z. Liu, J. Cheng, *Angew. Chem. Int. Ed.* **2019**, *58*, 4356–4360; *Angew. Chem.* **2019**, *131*, 4400–4404; e) B. Rösch, T. X. Gentner, H. Elsen, C. A. Fischer, J. Langer, M. Wiesinger, S. Harder, *Angew. Chem. Int. Ed.* **2019**, *58*, 5396–5401; *Angew. Chem.* **2019**, *131*, 5450–5455; f) J. Martin, J. Eyselein, J. Langer, H. Elsen, S. Harder, *Chem. Commun.* **2020**, *56*, 9178–9181.
[21] D. Schuhknecht, T. P. Spaniol, Y. Yang, L. Maron, J. Okuda, *Inorg. Chem.* **2020**, *59*, 9406–9415.
[22] a) D. S. Hutchings, P. C. Junk, W. C. Patalinghug, C. L. Raston, A. H. White, *J. Chem. Soc. Chem. Commun.* **1989**, 973–974; b) L. He, J. Cheng, T. Wang, C. Li, Z. Gong, H. Liu, B.-B. Zeng, H. Jiang, W. Zhu, *Chem. Phys. Lett.* **2008**, *462*, 45–48; c) M. D. Walter, G. Wolmershäuser, H. Sitzmann, *J. Am. Chem. Soc.* **2005**, *127*, 17494–17503; d) F. M. Sroor, L. Vendier, M. Etienne, *Dalton Trans.* **2018**, *47*, 12587–12595.
[23] M. S. Hill, M. F. Mahon, A. S. S. Wilson, C. Dinoi, L. Maron, E. Richards, *Chem. Commun.* **2019**, *55*, 5732–5735.
[24] R. Shannon, *Acta Crystallogr. Sect. A* **1976**, *32*, 751–767.
[25] A. L. Allred, *J. Inorg. Nucl. Chem.* **1961**, *17*, 215–221.
[26] a) B. Rösch, T. X. Gentner, J. Langer, C. Färber, J. Eyselein, L. Zhao, C. Ding, G. Frenking, S. Harder, *Science* **2021**, *371*, 1125–1128; b) M. Wiesinger, B. Rösch, C. Knüpfer, J. Mai, J. Langer, S. Harder, *Eur. J. Inorg. Chem.* **2021**, 3731–3741.
[27] a) L. Garcia, M. D. Anker, M. F. Mahon, L. Maron, M. S. Hill, *Dalton Trans.* **2018**, *47*, 12684–12693; b) D. Schuhknecht, T. P. Spaniol, I. Douair, L. Maron, J. Okuda, *Chem. Commun.* **2019**, *55*, 14837–14839; c) P. Stegner, C. Färber, J. Oetzel, U. Siemeling, M. Wiesinger, J. Langer, S. Pan, N. Holzmann, G. Frenking, U. Albold, B. Sarkar, S. Harder, *Angew. Chem. Int. Ed.* **2020**, *59*, 14615–14620; *Angew. Chem.* **2020**, *132*, 14723–14728.
[28] Deposition Number(s) 2112938 (for **3a**), 2112939 (for **3b**), 2112940 (for **4a**), 2112941 (for **5**), 2112942 (for **6**), 2112943 (for **8**), 2112944 (for **9**) contain the supplementary crystallographic data for this paper. These data are provided free of charge by the joint Cambridge Crystallographic Data Centre and Fachinformationszentrum Karlsruhe Access Structures service www.ccdc.cam.ac.uk/structures.

Manuscript received: November 11, 2021
Accepted manuscript online: December 7, 2021
Version of record online: January 14, 2022